New Progress in VLBI Tracking of GNSS Satellites at GFZ

L. Liu[1,2], R. Heinkelmann[1], V. Tornatore[3], R. Haas[4], A. Neidhardt[5], D. Duev[6], J. Kodet[7], J. Li[2], T. Nilsson[1], M. Xu[1,2], C. Plötz[5], U. Schreiber[7], S. Pogrebenko[6], G. Kronschnabl[5], J.A. Mora-Diaz[1], B. Soja[1], M. Karbon[1], C. Lu[1], V. Raposo-Pulido[1], H. Schuh[1]

Abstract The topic of VLBI tracking of GNSS satellites has lately emerged as a new way for linking the dynamic reference frame realized by GNSS satellites to the ICRF. Recently, a few related experiments and studies were carried out to test and further develop this technique. In this contribution, we present preliminary results of post-correlation with the observations from a recent VLBI tracking of a GLONASS satellite experiment performed by the radio telescopes in Wettzell and Onsala in January 2013 [1]. To determine and evaluate the ability of these observations, the appropriate way to fringe fit the correlation data from artificial signals is studied, and some graphs after calibrations from AIPS are analyzed.

Keywords GLONASS, VLBI satellite tracking, GNSS, clock model, fringe-fitting, narrow band, AIPS, calibration

1. Helmholtz Centre Potsdam, GFZ German Research Centre for Geosciences, Potsdam, Germany
2. Shanghai Astronomical Observatory, Chinese Academy of Sciences, Shanghai, China
3. Politecnico di Milano, DIIAR, Sezione Rilevamento, Milano, Italy
4. Chalmers University of Technology, Onsala Space Observatory, Onsala, Sweden
5. Federal Agency for Cartography and Geodesy, Geodetic Observatory Wettzell, Germany
6. Joint Institute for VLBI in Europe, The Netherlands
7. Technische Universität München, Geodetic Observatory Wettzell, Germany

1 Introduction

While the ITRF (International Terrestrial Reference Frame) is realized by the combination of the various space geodetic techniques, VLBI (Very Long Baseline Interferometry) is the only technique to determine the ICRF (International Celestial Reference Frame) through its observations of extragalactic radio sources. According to combinations of parameters derived by GNSS (Global Navigation Satellite Systems) and VLBI, e.g. troposphere delays [2], gradients, and UT1–UTC [3], evidence of discrepancies between the two systems becomes obvious. Terrestrial local ties can provide a way to interlink the otherwise independent technique-specific terrestrial reference frames, but only to some degree [4]. It is evident that errors in the determination of the terrestrial ties, e.g. due to the errors during the transformation from the locally surveyed coordinates into global Cartesian three dimensional coordinates, introduce significant errors in the combined analysis of space geodetic techniques. A new concept for linking the space geodetic techniques might be to introduce celestial ties, e.g. realized by several techniques co-located on board a satellite [5]. A small satellite carrying various space geodetic techniques is under investigation at GFZ. Such a satellite would provide a new observing platform with its own additional unknowns, such as the orbit or atmospheric drag parameters. A link of the VLBI and GNSS techniques might be achieved in a more direct way as well: by VLBI tracking of GNSS satellites with the extragalactic radio sources nearby as calibrators. This new kind of hybrid VLBI–GNSS observation could comprise a new direct inter-technique tie without the involvement of surveying methods and would improve the consistency of the two space

geodetic techniques VLBI and GNSS, in particular of their celestial frames. Several tests of this type of observation were already successfully carried out. First results were obtained from the GLONASS satellites tracking data in cooperation with JIVE using the software SWSpec and SCTracker [6]. In our work, to test this kind of innovative observation, we also analyzed the observations from an experiment where the PR09 GLONASS satellite was tracked [1] in this work.

2 "VLBI Tracking GLONASS" Experiment Description

With the new L-band receiver equipped at the 20-m Wettzell telescope [7], the PR09 GLONASS satellite was successfully tracked from 13:15:00 UT to 13:59:59 UT on January 28th, 2013 for the first time together with the 25-m Onsala telescope (experiment G130128, Figure 1 and Figure 2) [1]. Data were recorded in L1 format with 8 MHz bandwidth and RHCP (Right Hand Circular Polarization) [7] and correlated with the JIVE Software Correlator SFCX in the Nertherlands, which is based on the original design developed for VLBI tracking of the Huygens Probe. It is able to support both the far-field and the near-field delay models and processing data in various "flavors" of the Mark 5 format [8].

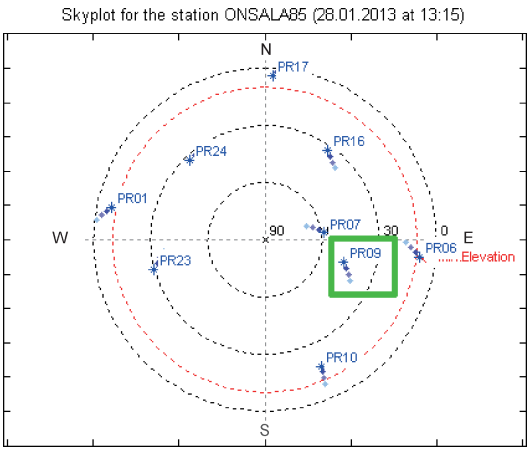

Fig. 1 Skyplot for station Onsala85.

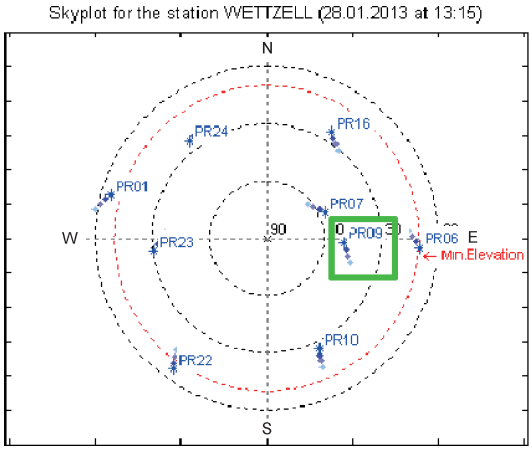

Fig. 2 Skyplot for station Wettzell.

3 Data Reduction for Artificial Signals

The artificial GLONASS signals are quite narrow, which differs from the broad continuous spectrum from natural extragalactic radio sources. The spectral resolution of the narrow band observations from GLONASS is 15.6 Hz, i.e., 512 channels per IF (Intermediate Frequency). The lower edge frequencies in the four IFs are displayed in Table 1 [9]. The whole bandwidth spreads from 1595 MHz to 1603 MHz. This situation limits the observation accuracy, and multi-band delays (the derivation of the phases over the wide-spreading bandwidth in different IFs with respect to the frequencies) could not be derived because the signals are all centered to almost the same frequency and differ only by 10 kHz. After correlation, the data were stored in files of the FITS-IDI (Flexible Image Transport System-Interferometry Data Interchange) [10] format with 0.5 s and 1 s integration time, respectively. To get the delay and rate for the geodetic parameter estimation, fringe-fitting should be done first.

Table 1 The lower edge IF frequencies (in MHz).

Pass	IF 1	IF 2	IF 3	IF 4
Frequency	1594.87	1594.88	1594.89	1594.90

3.1 Fringe-fitting

The aim of fringe-fitting is to get the delay and the rate, and the basic theory is as follows,

$$\Delta\phi_{t,v} = \phi_0 + (\frac{\partial\phi}{\partial\nu}\Delta\nu + \frac{\partial\phi}{\partial t}\Delta t) \quad (1)$$

$\frac{\partial\phi}{\partial\nu}$ denotes the delay, and $\frac{\partial\phi}{\partial t}$ is the rate [11]. The fringe-fitting was conducted by the Astronomical Imaging Processing System (AIPS), developed and maintained by NRAO. The algorithm determining the residual delay, rate, and phase in the AIPS software is realized by the task 'FRING'. Through FFT (Fast Fourier Transform) and least squares solution, single-band group delays and rate residuals were independently obtained from each of the four IFs. In the comparison between the results from 0.5 s and 1 s integration times, we set Wettzell as the reference station and chose the solution interval of 15 s (antenna stop and go in every 15 s [1]).

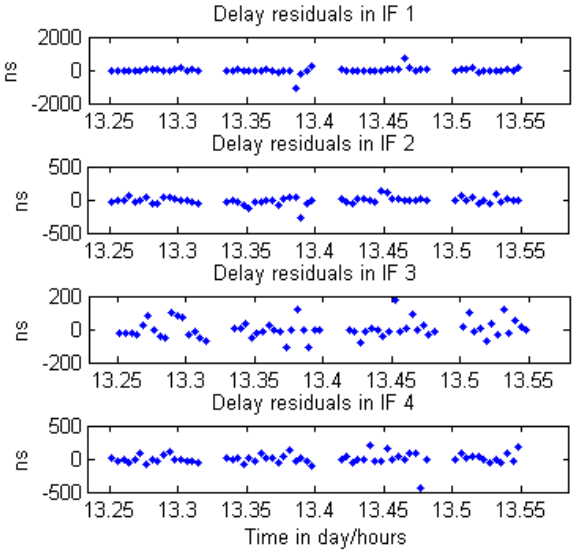

Fig. 3 Delay residuals correlation data with 1 s integration time.

From Figure 3, it is obvious that big outliers (IF 1) exist in delay residuals from the FITS-IDI data with 1 s integration time, while the 0.5 s FITS-IDI data improve the results by almost one order of magnitude (Figure 4). The delay residuals at a level of 10 ns in Figure 4 could come from the difference between the observations and the a priori delay model, the instrument,

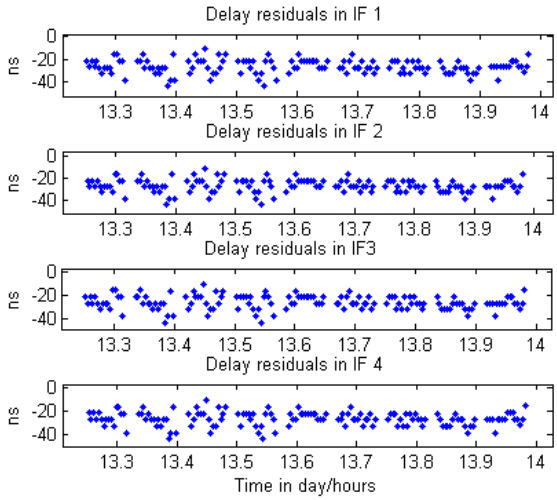

Fig. 4 Delay residuals correlation data with 0.5 s integration time.

the clock, etc. The delay residuals are below zero, indicating that there are some systematic errors which need further analysis. Results with a smaller integration interval, i.e., 0.25 s, were also tested and analyzed in [1]. In the fringe-fitting for the 0.5 s FITS-IDI data, the SNR cutoff is 10 dB.

$$\Delta\tau \sim \frac{1}{2\Delta\nu}\frac{1}{SNR} \quad (2)$$

$\Delta\nu$ is the bandwidth (8 MHz). We can tell from Equation 2 that the delay accuracy should be less than 6 ns. Through the fringe-fitting, the results were fitted to the midpoint of the epoch. The RMS of the phase, delay and rate with different solution intervals in the first scan are presented in Figure 5. The solution interval of 15 s (30 integrations) shows the best stability and highest precision. The average RMS (Root Mean Square) of the phase, delay, and rate are 1.43 degrees, 0.98 ns, and 0.34 mHz, and the SNR is 40.28 dB if we set the solution interval to 15 s. In conclusion, a smaller solution interval in the fringe-fitting lowers the accuracy with the SNR decreasing, while the larger solution intervals such as 30 s may have less stability, which is possibly caused by the rapid movements of the satellite. In a real time satellite tracking experiment, a small solution interval, i.e., 3 s could be more suitable with the correspondingly relatively lower average precision of 2.3 ns for delay residuals.

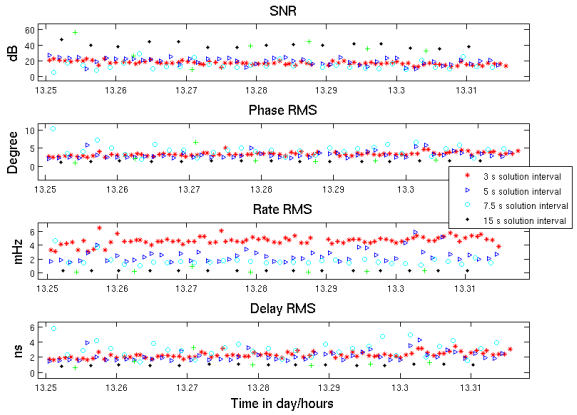

Fig. 5 SNR and RMS of phase, rate, and delay with different solution intervals.

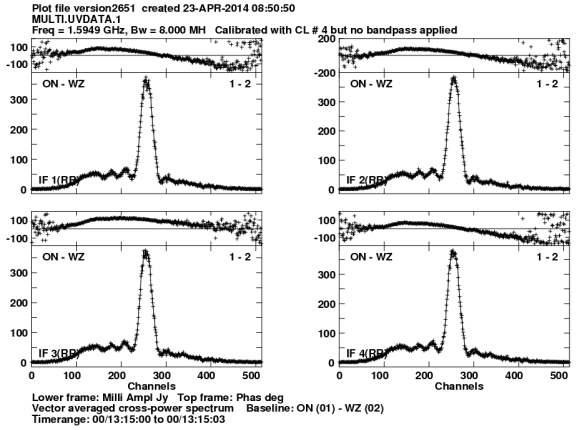

Fig. 7 Cross-power spectrum and phase against frequency with 3 s solution interval.

3.2 Calibrations and Graphic Analysis

There are several calibrations in AIPS, which are important for imaging, such as amplitude calibration, band pass calibration, self-calibration, etc. The task 'CLCAL' can apply the SN table from fringe-fitting to the CL table for the calibration [12]. With these calibrations, we can plot the results by the 'POSSM' task to present the cross-power spectrum and phase against frequency. The graphics in Figure 6 and Figure 7 show that the correlation process and fringe-fitting were successful.

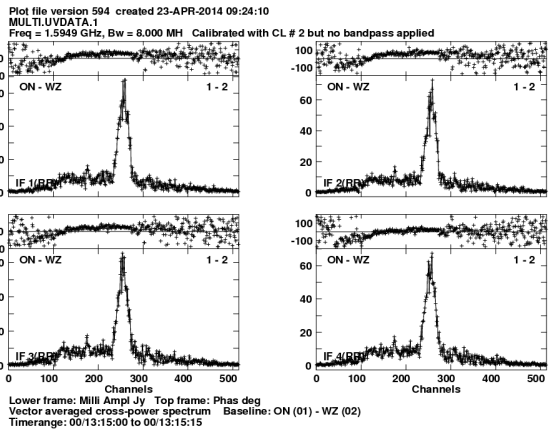

Fig. 6 Cross-power spectrum and phase against frequency with 15 s solution interval.

From Figure 6 and Figure 7, we can see that the smaller solution interval in fringe-fitting can cause a stronger amplitude and less noise in the results, while the delay (phase vs. frequency) is not as flat as that of a larger solution interval, which means that the delay residuals have some kind of deviations. To take into account the graphic results and the above mentioned RMS, a 15 s solution interval could be suitable for precise processing in VLBI satellite tracking.

4 Conclusions

Fringe-fitting with results of 0.5 s integration time is better than with 1 s integration time. The delay residuals improve by one order of magnitude. Precision of a level of 10 ns is obtained in the former case. The figures of cross-power spectrum and phase against frequency verify the reliability of the correlation and fringe-fitting in AIPS. A solution interval of 15 s is suitable in fringe-fitting in this experiment with FITS-IDI data of 0.5 s integration time; the corresponding RMS for phase, delay, and rate are 1.43 degrees, 0.98 ns, and 0.34 mHz. A small solution interval such as 3 s may be useful for real-time tracking. More data from future similar experiments with more stations are needed. Extending the observation duration and observing more satellites would also help to improve the results. Radio sources as calibrators with broader bandwidth added into GNSS tracking experiments may improve the GNSS observation accuracy.

References

1. Haas R., A. Neidhardt, J. Kodet, C. Plötz, U. Schreiber, G. Kronschnabl, S. Pogrebenko, D. Duev, S. Casey, I. Marti-Vidal, J. Yang, L. Plank. The Wettzell-Onsala G130128 experiment, *IVS 2014 General Meeting Proceedings*, this volume, 2014
2. Krügel, M., D. Thaller, V. Tesmer, M. Rothacher, D. Angermann, R. Schmid. Tropospheric parameters: combination studies based on homogeneous VLBI and GPS data. *Journal of Geodesy*, 81(6–8), doi: 10.1007/s00190-006-0127-8, 515–527, 2007
3. Thaller, D., M. Krügel, M. Rothacher, V. Tesmer, R. Schmid, D. Angermann. Combined Earth orientation parameters based on homogeneous and continuous VLBI and GPS data. *Journal of Geodesy*, 81(6-8), doi: 10.1007/s00190-006-0115-z, 529–541, 2007
4. Ray, J. and Z. Altamimi. Evaluation of co-location ties relating the VLBI and GPS reference frames. *Journal of Geodesy*, 79(4–5), doi: 10.1007/s00190-005-0456-z, 189–195, 2005
5. Tornatore, V., R. Haas, S. Casey, D. Duev, S. Pogrebenko, G. Molera Calvés. Direct VLBI Observations of Global Navigation Satellite System Signals, *Earth on the Edge: Science for a Sustainable Planet*, 139, doi: 10.1007/978-3-642-37222-3_32247-252, ISBN (online): 978-3-642-37221-3, 247-252, 2014
6. Tornatore, V., R. Haas, et al. Single baseline GLONASS observations with VLBI: data processing and first results. *Proceedings of the 20th Meeting of the European VLBI Group for Geodesy and Astrometry*, 162–165, 2011
7. Kodet, J., K.U. Schreiber, Ch. Plötz, A. Neidhardt, G. Kronschnabl, R. Haas, G. Molera Calvés, S. Pogrebenko, M. Rothacher, B. Maennel, L. Plank, A. Hellerschmied. Colocations of Space Geodetic Techniques on Ground and in Space. *IVS 2014 General Meeting Proceedings*, this volume, 2014
8. Duev, D. A., G. Molera Calvés, S. V. Pogrebenko, L. I. Gurvits, G. Cimó, and T. B. Bahamon. Spacecraft VLBI and Doppler tracking: algorithms and implementation. *Astronomy & Astrophysics*, 541, doi: 10.1051/0004-6361/201218885, 2012
9. Petrov, L., D. Gordon, J. Gipson, D. MacMillan, C. Ma, E. Fomalont, R. C. Walker, C. Carabajal. Precise geodesy with the Very Long Baseline Array. *Journal of Geodesy*, 83(9), doi: 10.1007/s00190-009-0304-7, 859–876, 2009
10. Greisen, E., The FITS Interferometry Data Interchange Convertion. AIPS Memo114r, 2011
11. Cotton, W. D., Fringe fitting. *Very Long Baseline Interferometry and the VLBA ASP Conference Series*, 82, 1995
12. Moran, J. M., Dhawan, V. An Introduction to Calibration Techniques for VLBI. *Very Long Baseline Interferometry and the VLBA ASP Conference Series*, 82, 161–188, 1995